

Atmospheric shower fluctuations and the constant intensity cut methodJaime Alvarez-Muñiz,^{*} Ralph Engel,[†] T. K. Gaisser, Jeferson A. Ortiz,[‡] and Todor Stanev
Bartol Research Institute, University of Delaware, Newark, Delaware 19716

(Received 12 September 2002; published 27 December 2002)

We explore the constant intensity cut method that is widely used for the derivation of the cosmic ray energy spectrum, for comparisons of data obtained at different atmospheric depths, for measuring average shower profiles, and for estimates of the proton-air cross section from extensive air shower data. The constant intensity cut method is based on the selection of air showers by charged particle or muon size and therefore is subject to intrinsic shower fluctuations. We demonstrate that, depending on the selection method, shower fluctuations can strongly influence the characteristics of the selected showers. Furthermore, a mixture of different primaries in the cosmic ray flux complicates the interpretation of measurements based on the method of constant intensity cuts. As an example we consider data published by the Akeno Collaboration. The interpretation of the Akeno measurements suggests that more than 60–70 % of cosmic ray primaries in the energy range 10^{16} – 10^{17} eV are heavy nuclei. Our conclusions depend only weakly on the hadronic interaction model chosen to perform the simulations, namely SIBYLL and QGSJET.

DOI: 10.1103/PhysRevD.66.123004

PACS number(s): 96.40.Pq, 13.85.–t, 96.40.–z

I. INTRODUCTION

Measuring extensive air showers (EAS) is currently the only way to study the cosmic ray spectrum and chemical composition at energies above 10^{14} eV, as well as the basic properties of hadronic interactions at \sqrt{s} above 1.8 TeV.

EAS can be detected with air shower arrays which measure densities of shower particles such as electrons, muons, photons, and sometimes hadrons arriving at the detector. These densities are typically fit to lateral distribution functions to derive the total number of charged particles, electrons N_e and muons N_μ at detector level. The particle numbers are functions of the primary cosmic ray energy E and the mass number A of the primary particle, and depend on the atmospheric depth of the observation level. At energies $E \geq 10^{17}$ eV the shower evolution can also be directly observed by measuring the fluorescence light from the atmospheric nitrogen that is excited by the ionization of the charged shower particles. In the following we will concentrate on air shower arrays. Imaging methods such as fluorescence or Cherenkov light techniques will be discussed elsewhere [1].

One of the classical methods in the analysis of air shower data is the constant intensity cut method. The idea is based on the fact that, due to the isotropy of the primary cosmic ray flux, showers generated by primary particles of the same energy and composition will arrive at the detector with the same frequency, assuming 100% detection efficiency. Selecting showers arriving at the detector with the same frequency under different zenith angles allows the measurement of the mean longitudinal shower profile. At large atmospheric depths after shower maximum, the shower size decreases

approximately exponentially with depth with a length scale commonly referred to as the *attenuation* length.

On the other hand, selecting showers with the same features (i.e. shower size, muon size etc.) at observation level and different incident angles allows the measurement of the *absorption* length which determines how the flux of the selected showers decreases with atmospheric depth.

Measurements of the attenuation length are commonly used to correct observed particle densities to those of equivalent vertical showers. By unfolding the geometry-related attenuation of showers an experiment can use the measured intensities of showers with fixed size to derive the primary all-particle flux.

The absorption length is inherently related to the mean free path of the EAS initiating primary particle. For example, the rate of proton air showers having the first interaction point (X_{int}) at a slant depth greater than X decreases as $\exp(-X/\lambda_{\text{int}})$, where λ_{int} is the mean free path for p -air collisions. On this basis, several methods of extracting the p -air cross section [23] from measurements of EAS have been applied in air shower experiments [2–7].

Air shower arrays cannot measure the depth of the first interaction of the primary particle generating the observed shower, which directly relates to the mean free path. The decrease with zenith angle of the frequency of showers having the same electron N_e and muon N_μ sizes at observation level is studied instead. In the absence of intrinsic shower fluctuations these measurements would reflect the depth distribution of primary interactions. However, the longitudinal development of showers is itself subject to large fluctuations. To disentangle these fluctuations from those of the first interaction point is not an easy task.

This problem is usually addressed by introducing a coefficient (k) which relates the observed shower absorption length (Λ_{obs}) and the inelastic cross section through the equation $\Lambda_{\text{obs}} = k \times \lambda_{\text{int}}$ [8]. The numerical value of k has to be obtained from simulations of EAS. The coefficient k reflects the influence of the features of the hadronic interactions model on the fluctuations in the shower development.

^{*}Electronic address: alvarez@bartol.udel.edu[†]Present address: Forschungszentrum Karlsruhe, Institut für Kernphysik, Postfach 3640, 76021 Karlsruhe, Germany.[‡]Present address: Instituto de Física “Gleb Wataghin,” Universidade Estadual de Campinas 13083-970 Campinas-SP, Brazil.

The value of k depends on the cross sections, secondary particle multiplicity and elasticity in the hadronic interaction model. Due to the necessary extrapolation of hadronic multiparticle production to unmeasured regions of the phase space and to high energy, the extracted cross section becomes model dependent.

Further difficulties in determining the inelastic p-air cross section from EAS measurements are related to experimental uncertainties and limitations in the determination of the development of air showers, and also to the fact that the cosmic ray flux might be “contaminated” with primaries heavier than protons which in principle tend to decrease the observed mean free path.

In this article we shall study the importance of intrinsic shower fluctuations for the experimentally observed attenuation and absorption lengths by considering two examples: (i) the reconstruction of the primary cosmic ray spectrum using charged particle shower sizes, and (ii) the measurement of the proton-air cross section, following closely the method applied first by the Akeno group [2,4] which we call the constant N_μ, N_e method.

In the process of (ii) we found that the Akeno observations can best be understood if there is a large fraction of heavy nuclei present in the cosmic ray beam from 10 to 100 PeV.

The paper is structured as follows. In Sec. II we study the possible errors introduced in the derivation of the primary cosmic ray spectrum by shower fluctuations when the constant intensity method is applied. Section III consists of three parts. Section III A summarizes the basics of the constant $N_e - N_\mu$ method. In Sec. III B we describe the predictions of this method for proton induced showers and in Sec. III C we discuss the more realistic situation of a mixed primary cosmic ray composition. Section IV concludes the paper.

II. DERIVATION OF THE COSMIC RAY ENERGY SPECTRUM

The constant intensity cut method has been used for studies of the primary cosmic ray spectrum for at least 40 years. Let us give as an example the interpretation of the results of the BASJE air shower array at Mt. Chacaltaya performed in 1965 [9]. Since Mt. Chacaltaya is at an altitude of 5220 m above sea level (540 g/cm² depth), the shower size distributions obtained with the constant intensity cut could be used to estimate the size of the showers at shower maximum. Under the assumption that the size at maximum is proportional to the primary energy E , this gave directly the primary energy spectrum within a constant which was estimated to be ~ 2 GeV/particle at shower maximum.

In this work we apply the constant intensity cut method in a different way, similar to what more contemporary experiments do (see for instance [10]).

For illustrative purposes we first apply the method assuming the primary spectrum is composed of pure protons. We have simulated proton-induced showers at zenith angles $\theta = 0^\circ, 15^\circ, 30^\circ$ and 45° down to the altitude of the Akeno array, corresponding to a vertical depth of $X_v = 920$ g/cm². Shower energies were drawn from an E^{-3} differential injection

TABLE I. Results of the fit to the relation between shower energy and size at observation level for vertical showers at different depths X_v and assuming different cosmic ray primaries. The last row corresponds to the energy-shower size relation obtained for a mixed composition assuming equal fractions of p, He, CNO and Fe. The function used to do the fit is $E = \hat{E}(N_e^0)^{(1-\epsilon)}$.

Primary	X_v (g/cm ²)	$\log_{10}(\hat{E}/\text{eV})$	ϵ
p	700	9.29	0.019
p	870	9.81	0.072
p	920	9.91	0.077
He	920	10.07	0.089
CNO	920	10.24	0.103
Fe	920	10.63	0.143
mixed	920	10.21	0.103

spectrum in the energy range between 10^{16} and 10^{18} eV.

We used a hybrid air shower simulation program to generate large samples of showers in an efficient and fast manner [11]. The hybrid method consists of calculating shower observables by a direct simulation of the initial part of the shower, tracking all particles of energy above $E_{\text{thr}} = 0.01 E$. Presimulated showers for all subthreshold particles are then superimposed after their first interaction point is simulated. The subshowers are described with parametrizations that give the correct average behavior, and at the same time describe the fluctuations in shower development of both electrons and muons.

The procedure we use to reconstruct the primary spectrum is the following. First, from the simulations we obtain the relation between shower energy (E) and shower size at observation level in vertical showers (N_e^0). This relation is given in Table I. Our simulations predict the shower size spectra at Akeno level for different zenith angles, and we treat them as if they were actual experimental data, replacing the detector induced fluctuations in $\log_{10} N_e$ by a Gaussian resolution function of width $\Delta \log_{10} N_e = 0.05$. Since we do not simulate showers of energy below 10^{16} eV there is an artificial break in the size spectra at low energy. To avoid it we choose $N_e = 10^7$ as a threshold value above which our “array” is fully efficient, and we only deal with showers having N_e above this value.

We apply cuts at constant shower intensity, and by studying the decrease with zenith angle of the size corresponding to each intensity, we obtain the shower attenuation length, which we use to estimate the shower size at $\theta = 0^\circ$ from the known size at zenith angle θ . (We checked that the attenuation length obtained from the simulated data in this way agrees with the attenuation length of the averaged profile of the input showers.) This is the classical integral application of the method. Given N_e^0 we can use the previously obtained relation between E and N_e^0 to estimate the energy of each individual shower. The energy spectrum for different zenith angles can then be reconstructed and compared to the injected spectrum. Figure 1 shows the shower energy resolution we achieve with this procedure. The distribution of differences between reconstructed and injected energies is

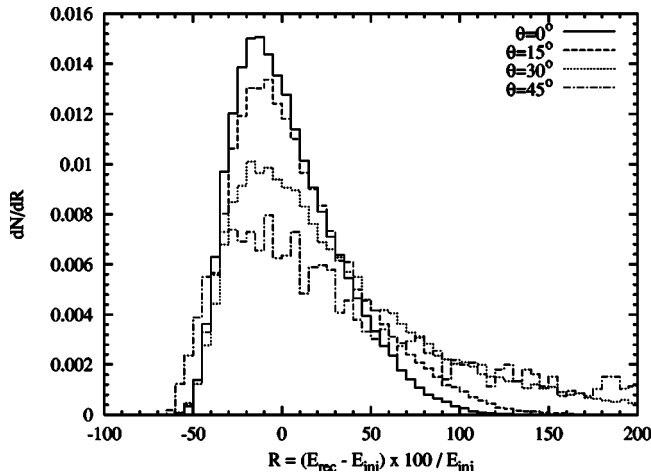


FIG. 1. Energy resolution of proton-induced showers for different zenith angles. The SIBYLL 2.1 hadronic generator code was used to simulate the showers.

highly asymmetric. The asymmetry depends on zenith angle as showers at larger zenith angles are further away from their maximum where the fluctuations in shower size are smallest. There is a clear tendency to misreconstruct showers of a certain injected energy assigning them a higher energy.

In Fig. 2 we compare the reconstructed and injected spectra for different zenith angles. The spectra are multiplied by $E^{2.5}$ for a better resolution. Although we draw showers from an E^{-3} differential spectrum, the cut in N_e decreases the contribution of the lower energy cosmic rays and creates the turnaround seen in Fig. 2. The larger the zenith angle, the higher the shower energy must be to exceed the N_e cut, producing a strongly zenith angle dependent energy cut.

Besides, as mentioned previously, with increasing zenith angle the shower is sampled further away from shower maximum and the fluctuations in N_e grow, producing a broadening of the injected spectrum. These two effects, however, vanish almost completely in the reconstructed spectra.

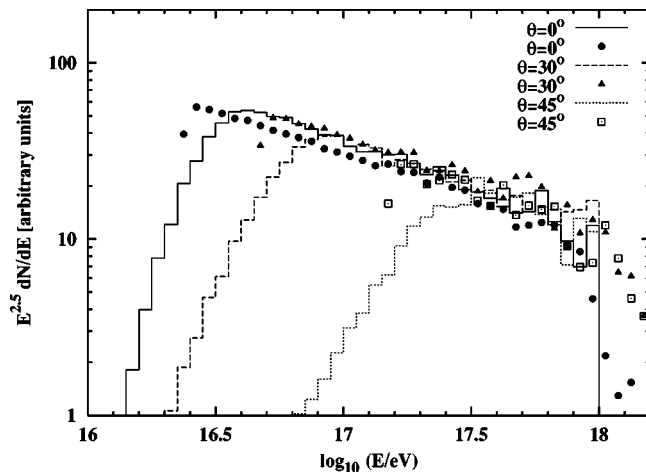


FIG. 2. Reconstructed (points) and injected (histograms) energy spectra (multiplied by $E^{2.5}$ at different zenith angles). Note that larger zenith angles contribute to the derived cosmic ray spectrum in a limited energy range because of the $N_e > 10^7$ threshold.

Imposing a cut in N_e produces a corresponding cut in E through the relation between energy and size at observation level. In our case $N_e > 10^7$ implies that $\log_{10} E > 16.36, 16.66, 17.16$ at zenith angle $0^\circ, 30^\circ$ and 45° respectively. As a consequence all the low energy injected events are reconstructed with energies above these values, and they pile-up rendering a simple power law. A fit to the reconstructed spectra reveals that the differential spectral index decreases by only about 2–3%. This is an important effect which should be present in experiments reconstructing the spectrum which use a relation between shower energy and shower size at observation depth, for instance at a certain distance from the core of the shower. Although the spectral shape is preserved almost completely there is a slight, but noticeable difference in the absolute normalization of the spectra reconstructed from showers at different zenith angles. The energies derived from showers at nonvertical angle are always overestimated, which leads in principle to an artificially increased normalization. Figure 2 shows that increase for an angle of 30° , however the normalization from the 45° showers is again lower. This may be due to the energy resolution distribution that peaks well below 0 for these showers. Independently of the exact reason for the changing normalization, Fig. 2 demonstrates that the exact energy derivation depends strongly on the shape of the shower fluctuations. Since these fluctuations change with the atmospheric depth, so does the reconstruction accuracy. As a whole, though, the method works quite well.

The reconstruction of the shower energy from N_e is affected even less by the shower fluctuations if the depth of the detector is close to the depth of shower maximum. In this case the danger is in the inclusion of showers that have not yet achieved their maximum development. Such showers may introduce a significant bias when their size is converted to vertical size by using the attenuation length. In the example discussed above, the mean depth of shower maximum is $\sim 650 \text{ g/cm}^2$ with a standard deviation of $\sim 70 \text{ g/cm}^2$, so that only a small fraction $\sim 0.5\%$ of the vertical showers have their maxima below observation level. This fraction is much smaller for inclined showers.

Further difficulties in the reconstruction arise in the more realistic case when the primary spectrum consists of a mixed composition of different nuclei. The heavier the primary nucleus, the further away is the observation level from shower maximum. From this point of view the spectrum reconstruction for a mixed primary composition is analogous to using proton showers to very large zenith angles.

To explore this point we have simulated a primary composition consisting of equal fractions of protons, He, CNO and Fe. We obtained the $E-N_e$ relation at 920 g/cm^2 (shown in Table I) from this particular mixture of nuclei, and applied the same procedure as before to reconstruct the primary spectrum. The reconstruction is again affected by the cut in N_e as explained above. The result is that both the spectral index and the normalization of the reconstructed spectrum differ from the corresponding values in the injection spectrum by only a few percent.

It is important to note that we have made use of our prior knowledge of the injected primary composition to recon-

struct the spectrum. We expect the reconstruction method to work either when the primary composition is known or when a composition independent energy estimator is used. (The density at 600 m from the cores of large showers is an example of a measure of shower energy chosen because of its relative insensitivity to primary mass [12].) We have checked that using the $E-N_e$ relation obtained for pure protons tends to underestimate the normalization of a mixed spectrum. The reason is that a shower of energy E initiated by a heavy nucleus has on average a smaller size at observation level than a proton shower of the same energy. A smaller energy is then assigned to the shower when the $E-N_e$ relation for protons is used. As expected, we observed the opposite behavior when the $E-N_e$ relation for pure iron (also shown in Table I) is used to reconstruct the mixed composition spectrum.

The most difficult case is obviously that of changing chemical composition. Because of the changes of the spectrum normalization for different primary nuclei the shape of the spectrum can also be derived incorrectly. The composition and spectrum then have to be reconstructed simultaneously from different shower parameters.

We conclude that the integral application of the constant intensity cuts method for the derivation of the primary cosmic ray spectrum works well when the cosmic ray composition is known. The use of wrong composition models can lead to erroneous conclusions for the energy spectrum, mostly in the determination of its normalization. The method is not strongly affected by the intrinsic fluctuations in the shower in the energy range we have explored.

III. THE CONSTANT N_e-N_μ METHOD

The total column density of atmosphere available for shower development increases with the incident angle θ as $\sec \theta$. The total number of electrons at a fixed slant depth after the shower maximum reflects the stage of evolution of the shower. If shower fluctuations were absent, selecting showers of fixed energy at different zenith angles which have the same electron size N_e , would *a priori* guarantee that they have developed through the same column of atmosphere between the first interaction point and observation level. The selected showers would only differ in the depth at which the first primary p-air interaction had occurred. The proton-air interaction length λ_{p-air} and the corresponding cross section σ_{p-air} would then be measured. The fact is, however, that N_e does have large fluctuations.

To address this problem and select showers of fixed primary energy, experiments often require that the showers have the same muon size at observation level N_μ . Unlike electrons, the number of muons N_μ remains almost constant after maximum, and hence it is a good estimator of the primary energy at essentially any observation depth below shower maximum. Selecting the showers with large electron sizes within the same N_μ bin increases the probability that they are induced by protons. The higher the size is, the lower is the contamination from heavier primaries.

Once showers are selected in this way, the frequency (f) of showers falling in a given (N_μ, N_e) bin is measured for dif-

ferent zenith angles. The ratio of the frequency of selected showers at two zenith angles (θ_1 and θ_2) is related to the observed absorption length by

$$R(\theta_1, \theta_2) = \frac{f(N_\mu, N_e, \theta_1)}{f(N_\mu, N_e, \theta_2)} = \exp\left[-\frac{X_v}{\Lambda_{\text{obs}}}(\sec \theta_1 - \sec \theta_2)\right], \quad (1)$$

where X_v is the vertical depth of the detector.

Clearly, intrinsic fluctuations of the shower profile will change the relation between the first interaction point and the electron and muon number at larger depths. In the following we will study how such fluctuations influence the observed absorption length, using detailed, up-to-date hadronic interactions models. For definiteness we will concentrate on the implementation of the method as used by the Akeno group [2,4]. A similar procedure was also used more recently by the EAS-TOP Collaboration [7].

A. Application to proton-induced showers

In general, the primary cosmic ray flux consists of nuclei of a variety of mass numbers. Since we want to study the constant N_e-N_μ method itself we simplify the problem and start with the assumption that all primary particles are protons. If the procedure does not give the correct cross section for a purely proton flux, the correct derivation for a mixed cosmic ray composition would be impossible.

We have performed simulations of proton-induced showers at several zenith angles and calculated the frequency of showers having N_μ muons and N_e electrons at observation level. The detector was chosen to be located at Akeno altitude, corresponding to a vertical depth of $X_v=920$ g/cm². Shower energies were drawn from an E^{-3} differential spectrum in the energy range between 10^{16} and 10^{18} eV. We performed the simulations for fixed zenith angles ($\theta=0^\circ$, 15° , 30° and 45°). We thus simplify the problem once again by neglecting the errors introduced by the experimental shower zenith angle reconstruction.

To study the dependence on the hadronic interaction model we have performed our simulations with two models, namely SIBYLL 2.1 [13,14] and QGSJET98 [15]. The two models give similar predictions for the shower development in the energy range $10^{16}-10^{18}$ eV [11]. As will be shown, our results depend only weakly on the choice of model.

For a realistic simulation of the observed shower parameters one should account for the experimental uncertainty and fluctuations due to the detector. A detailed simulation of the biases and efficiencies of the detectors is beyond the scope of this paper. It requires the use of specifically designed Monte Carlo programs of each particular ground array. We replace instead the detector induced fluctuations in $\log_{10}N_\mu$ and $\log_{10}N_e$ by Gaussian resolution functions of widths $\Delta \log_{10}N_\mu=0.1$ and $\Delta \log_{10}N_e=0.05$ respectively. These are the experimental errors reported by the Akeno group [4]. For each of the simulated showers modified $\log_{10}N_\mu$ and $\log_{10}N_e$ are sampled according to the theoretical

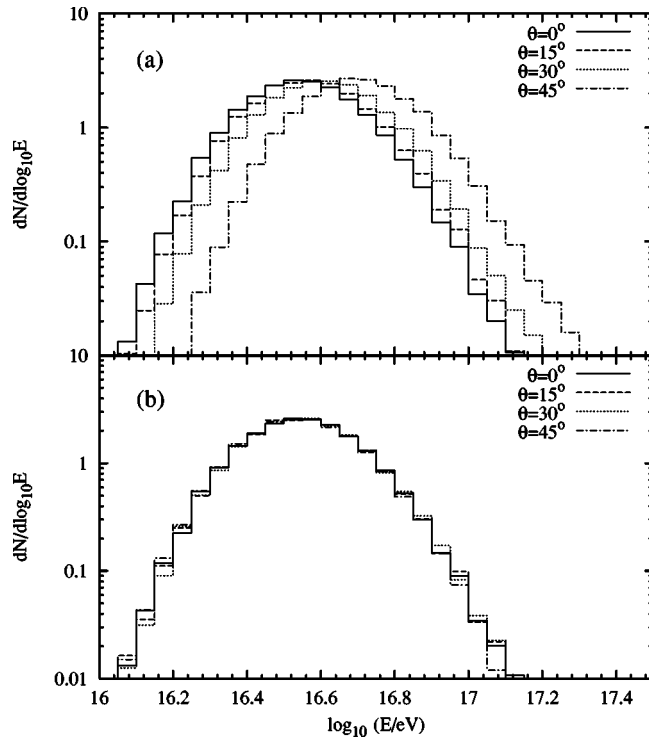


FIG. 3. Top panel: Simulated energy distribution of proton-initiated showers after applying the muon cut. The selected showers have $\log_{10}N_\mu$ between 5.25 and 5.45. The muons have energy above $E_\mu^{\text{thr}} = 1 \text{ GeV} \times \sec \theta$ at 920 g/cm^2 . The distribution is shown for different zenith angles. The SIBYLL 2.1 hadronic generator code was used to simulate the showers. Bottom panel: same as top panel after applying the constant intensity cut.

values and the detector resolution.

It is possible and even likely that, due to different energy thresholds and absorbing materials, the experimental definition of N_e does not coincide exactly with the corresponding quantity that the Monte Carlo generates. In such a case one should apply a correction factor to achieve a full reproduction of the experimental result. As we show further below, however, a possible small discrepancy in the definition of N_e would not alter the conclusions of this study.

We have simulated a sample of 500 000 proton showers, comparable to the statistics of the full event sample reported by the Akeno Collaboration in [4]. We apply the constant $N_e - N_\mu$ method by first selecting showers which have $\log_{10}N_\mu$ between 5.25 and 5.45 at observation level, the muon number of the first bin of the Akeno analysis [4]. Only muons with energy $E_\mu > 1 \text{ GeV} \times \sec \theta$, which is the muon energy threshold of the Akeno experiment [4], are considered. In the top panel of Fig. 3 we plot the energy distribution of showers selected after applying the muon cut. For fixed primary energy the mean muon number is smaller at large zenith angles as compared to vertical showers. This is due both to the dependence of the energy threshold on zenith angle, and to the increase of the probability for muon decay when the zenith angle increases and muons have to traverse more column depth of atmosphere. As a consequence, the energy distribution shows a dependence on zenith angle, i.e. selecting showers with the same number of muons does not

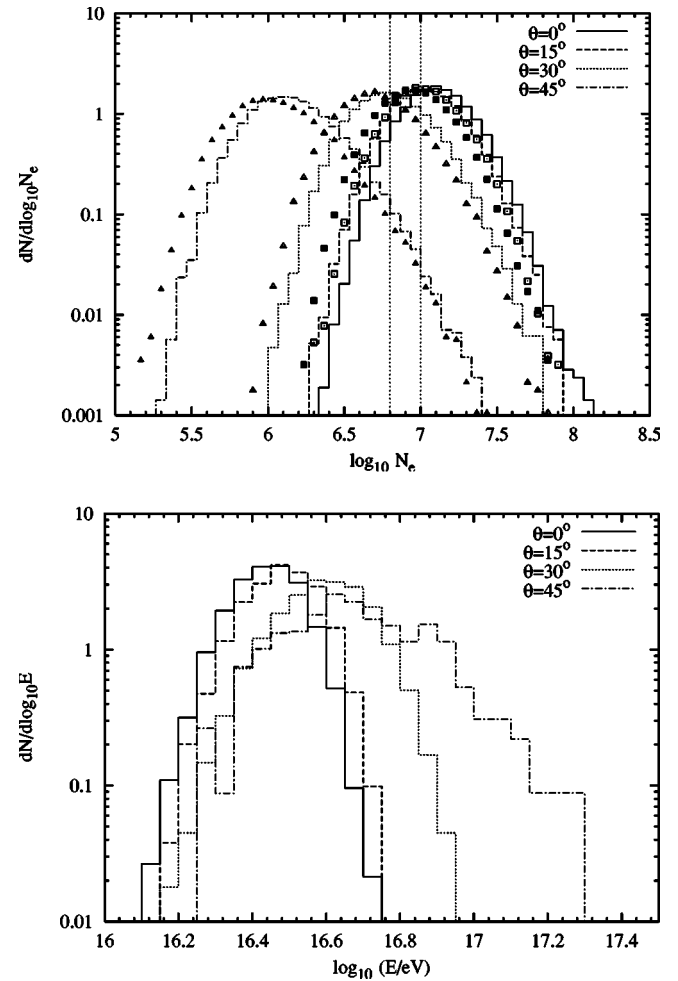


FIG. 4. Top panel: Shower size at 920 g/cm^2 depth in proton-initiated showers having between $10^{5.25}$ and $10^{5.45}$ muons at 920 g/cm^2 . The size distribution is shown for showers initiated at different zenith angles. Histograms correspond to showers simulated using SIBYLL 2.1, and points to showers simulated with QGSJET98. Bottom panel: Energy distribution of the showers falling in the N_e bin indicated by the vertical bars in the top panel.

perfectly guarantee that they have the same energy distribution. One can correct for the N_μ attenuation by the constant intensity cut method shifting slightly the $\log_{10}N_\mu$ bin so that the intensity of showers is the same at all zenith angles. This is equivalent to a correction of the shower muon longitudinal profile as a function of the zenith angle. The bottom panel of Fig. 3 shows the energy distribution of the selected showers after applying the constant intensity cut method. The constant intensity cut method works almost perfectly, giving a distribution of selected shower energies independent of zenith angle. The width of the shower energy distribution is determined by the width of the N_μ bin, and by the N_μ shower to shower fluctuations.

Once showers of the same energy have been selected, we select in addition showers with constant N_e , as was done by the Akeno team. The top panel of Fig. 4 shows the N_e spectra of showers having $\log_{10}N_\mu$ between 5.25 and 5.45 for the four nominal zenith angles. The two vertical lines mark the bin in $\log_{10}N_e$ chosen by the Akeno Collaboration to perform

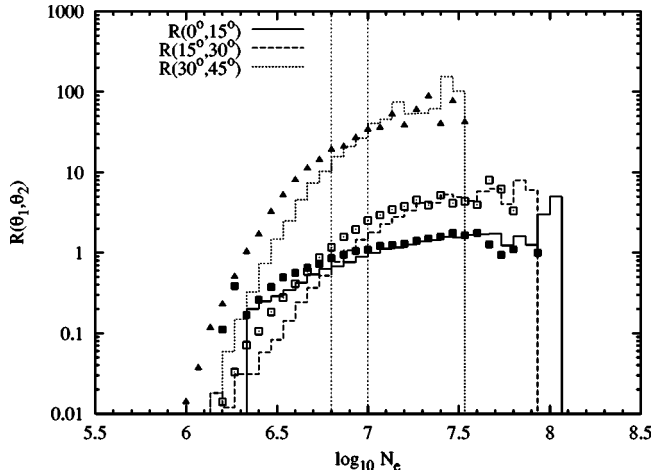


FIG. 5. Ratios of number of proton-initiated showers having between $10^{5.25}$ and $10^{5.45}$ muons and electron size N_e at 920 g/cm^2 as a function of N_e . Histograms correspond to showers simulated using SIBYLL 2.1, and points to showers simulated with QGSJET98.

their analysis of the showers in the $5.25\text{--}5.45$ bin in $\log_{10}N_\mu$. The bottom panel of Fig. 4 shows the energy distribution of showers in the selected N_e bin. It shows that the energy estimate that was very good after the N_μ bin selection with constant intensity cuts, is now again angle dependent.

We have compared the $N_e(E)$ dependence calculated by the Monte Carlo code to the experimental one used by the Akeno experiment [16]. In the $\log_{10}N_e$ bin $6.8 - 7.0$ the Akeno formula gives $\log_{10}(E/\text{eV}) = 16.40$ and the Monte Carlo code using SIBYLL 2.1 yields 16.43 . Both values are estimated at the center of the bin. The differences when using the $N_\mu(E)$ are higher. The Akeno Collaboration [16] derived $\log_{10}(E/\text{eV}) = 16.25$ in the $\log_{10}N_\mu$ bin $5.25\text{--}5.45$. SIBYLL 2.1 gives $\log_{10}(E/\text{eV}) = 16.55$ and QGSJET98 $\log_{10}(E/\text{eV}) = 16.48$ in the same $\log_{10}N_\mu$ bin.

In Fig. 5 we further illustrate this dependence by showing the frequency ratios of the showers in Fig. 4, in dependence of the selected electron size. The ratio is only plotted for adjacent zenith angles. It depends strongly on the N_e bin used for shower selection. According to Eq. (1) this ratio should be constant over a certain range in N_e for all different zenith angle combinations. Figure 5 shows that the N_e ranges where the ratio is approximately constant depend on the shower angle combination. For both SIBYLL 2.1 and QGSJET98 models they lie above $\log_{10}N_e$ of 7.4 for the $\log_{10}N_\mu$ bin $5.25\text{--}5.45$. The bin in N_e chosen by Akeno for the cross section analysis is clearly in a region where the intensity ratios depend strongly on N_e .

The ratio of two ratios R for different combinations of zenith angles can be used as a consistency check of the results. The expected values of the double ratio are [see Eq. (1)]

$$\frac{\log_{10}R(15^\circ, 30^\circ)}{\log_{10}R(0^\circ, 15^\circ)} = \frac{\sec(30) - \sec(15)}{\sec(15) - \sec(0)} \sim 3.4 \quad (2)$$

$$\frac{\log_{10}R(30^\circ, 45^\circ)}{\log_{10}R(0^\circ, 15^\circ)} = \frac{\sec(45) - \sec(30)}{\sec(15) - \sec(0)} \sim 7.4. \quad (3)$$

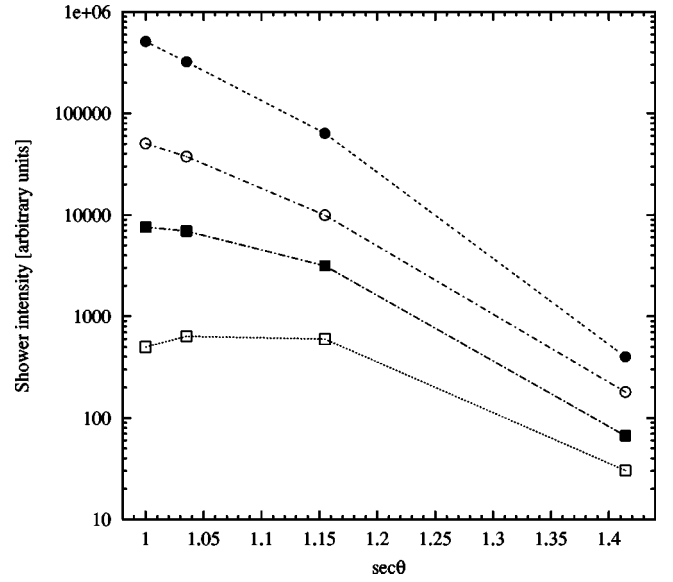


FIG. 6. Zenith angle dependence of the intensity of proton-induced showers having constant $\log_{10}N_\mu = 5.25\text{--}5.45$ and constant $\log_{10}N_e$ for different values of $\log_{10}N_e$. Empty squares $\log_{10}N_e = 6.8\text{--}7.0$, filled squares $\log_{10}N_e = 7.0\text{--}7.2$, empty circles $\log_{10}N_e = 7.2\text{--}7.4$ and filled circles $\log_{10}N_e = 7.4\text{--}7.6$. Showers were simulated with SIBYLL 2.1. The points are joined by straight lines to guide the eye. To avoid overlapping, the results for different N_e bins were multiplied by different arbitrary factors.

It is easy to verify that this is not the case for the selected showers falling in the bin in $\log_{10}N_e$ between 6.8 and 7.0 . These numbers are, however, the approximate scaling factors when comparing the plateaus of the ratios in Fig. 5. The figure suggests that zenith angle dependent bins in electron size should be used in order to get an angular-independent value of Λ_{obs} , provided of course the selected showers are initiated by protons as in our simulation.

A similar consistency check can be performed by plotting the observed shower intensity as a function of $\sec \theta$. Figure 6 shows the intensity of proton-initiated showers falling in the $\log_{10}N_\mu = 5.25\text{--}5.45$ bin for different N_e bins. The deviation from straight lines, which are expected for exponential attenuation of showers with $\sec \theta$, demonstrates that the constant $N_e - N_\mu$ method fails to select similar showers, unless a large value of N_e is selected. The intensity of the selected showers certainly does not decrease as $\exp(-X/\Lambda_{\text{obs}})$ in the $(\log_{10}N_\mu, \log_{10}N_e) = (5.25\text{--}5.45, 6.8\text{--}7.0)$ bin. Formal fits of the three higher N_e bins plotted in Fig. 6 give Λ_{obs} values of 138 ± 36 , 85 ± 8 and $68 \pm 3 \text{ g/cm}^2$ for $\log_{10}N_e$ of $7.0\text{--}7.2$, $7.2\text{--}7.4$ and $7.4\text{--}7.6$ respectively. Compared to the proton-air cross section of 456 mb in SIBYLL 2.1 these values lead to k values of 2.60 ± 0.67 , 1.61 ± 0.14 , and 1.28 ± 0.06 .

The analogous analysis carried out with QGSJET98 for the same muon number bin and $\log_{10}N_e = 7.4\text{--}7.6$ gives $\Lambda_{\text{obs}} = 69 \pm 2$ which corresponds to a k -factor of 1.26 ± 0.04 . Within the statistical uncertainty this value agrees with the one derived from SIBYLL 2.1 simulations. The weak model dependence is not unexpected. The energy of the showers considered here is only one order of magnitude higher than the equivalent energy of the Tevatron collider. Both models

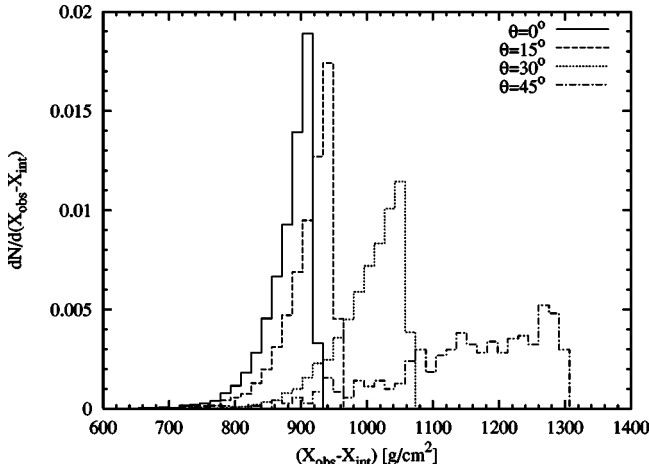


FIG. 7. Distribution in $X_{\text{obs}} - X_{\text{int}}$ of the showers that fall in the $(\log_{10}N_{\mu}, \log_{10}N_e) = (5.25 - 5.45, 6.8 - 7.0)$ bin.

were tuned to reproduce the Tevatron measurements and predict rather similar muon and electron numbers for $E \ll 10^{19}$ eV.

B. Shower fluctuations

The ultimate reason why the constant $N_e - N_{\mu}$ method does not work is that the discussed shower selection is dominated by the intrinsic fluctuations in shower development. This is illustrated in Fig. 7 in which we plot the distribution of “shower lengths” of showers with $(\log_{10}N_{\mu}, \log_{10}N_e) = (5.25 - 5.45, 6.8 - 7.0)$ for different angles. We arbitrarily define the shower length as the difference between the slant depth of observation level (X_{obs}) and the slant depth of the first interaction point. If the longitudinal shower profile were not biased by the selection criteria all four histograms would be very similar. They are instead very different and demonstrate that the selection is on the width of shower development rather than on the depth of the first interaction X_{int} . Indeed, for all angles most of the selected showers have their first interaction point near the top of the atmosphere. Even in the larger N_e bins the situation is not qualitatively different, as can be seen in Fig. 6.

In Table II we give the average values and the widths of the distributions shown in Fig. 7. For the method not to be dominated by intrinsic fluctuations, the average value of $X_{\text{obs}} - X_{\text{int}}$ should be independent of zenith-angle. The increase of atmospheric depth from $\theta = 0^\circ$ to 45° should lead to a shift of the first interaction point by about 400 g/cm^2 .

TABLE II. Average values and standard deviations (in parentheses) of the distributions of $X_{\text{obs}} - X_{\text{int}}$ (see also Fig. 7), $X_{\text{max}} - X_{\text{int}}$ and $X_{\text{obs}} - X_{\text{max}}$ for proton-initiated showers belonging to the $(\log_{10}N_{\mu}, \log_{10}N_e) = (5.25 - 5.45, 6.8 - 7.0)$ bin.

θ (deg)	X_{obs} (g/cm^2)	$(X_{\text{obs}} - X_{\text{int}})$ (g/cm^2)	$(X_{\text{max}} - X_{\text{int}})$ (g/cm^2)	$(X_{\text{obs}} - X_{\text{max}})$ (g/cm^2)
0	920.0	881.3 (35.7)	581.4 (31.1)	300.1 (42.6)
15	952.2	911.1 (37.6)	585.8 (31.6)	325.2 (42.3)
30	1062.3	1002.0 (50.6)	613.7 (39.5)	388.2 (51.3)
45	1301.1	1152.9 (109.7)	699.7 (95.1)	453.8 (92.5)

Due to the fluctuations the actual mean shift is only by about 110 g/cm^2 .

A way to quantify which part of the longitudinal shower development, namely the first few interactions or the latest interactions, contributes most to the fluctuation in shower length, is calculating the average values and widths of the distributions of $X_{\text{max}} - X_{\text{int}}$ and $X_{\text{obs}} - X_{\text{max}}$. This is shown in columns 3 and 4 in the table. The tail of the shower contributes more to the overall fluctuation in shower length than the first few interactions, although the contribution depends on the zenith angle. In terms of the ratio of $\sigma/\Delta X$ the angular dependence is bigger for $(X_{\text{obs}} - X_{\text{max}})$, where it changes from 0.054 for vertical showers to 0.136 for showers developing under 45° .

C. Composition

In contrast to our findings summarized in Fig. 6, the Akeno Collaboration reports a $\sec \theta$ dependence of the observed frequencies of showers selected by the constant $N_e - N_{\mu}$ method which is compatible with an exponential attenuation (see Fig. 1 in Ref. [4]). By looking at Figs. 4 and 6 it is clear that the intensity of proton showers in the nominal bin is not large enough at small zenith angles to produce a straight line. Proton showers penetrate too much in the atmosphere and thus have large electron sizes at observation level. In principle, this statement depends on the hadronic interaction model used in the simulations. A model which predicts the same muon number at lower shower energy can lead to an increase of the vertical shower intensity in the considered bin. However, simulations with QGSJET, which predicts the largest muon multiplicity among the contemporary hadronic interaction models, show that this conclusion is unchanged if the muon multiplicity in the considered energy range is increased by up to 20%.

A way to increase the intensity of the selected showers would be to “contaminate” the sample with heavy primaries. These give rise to showers which are less penetrating, shifting the distribution in electron size to smaller values. This is illustrated in the top panel of Fig. 8 for a primary composition consisting of 85% Fe, 10% CNO, 4% He and 1% protons. The bottom panel of Fig. 8 shows the contributions to the total electron size distribution from showers initiated by the different primaries. It is remarkable, and to our understanding a coincidence, that the tail of the total distribution in electron size has roughly the same slope as the tail of the contribution from proton-induced showers alone.

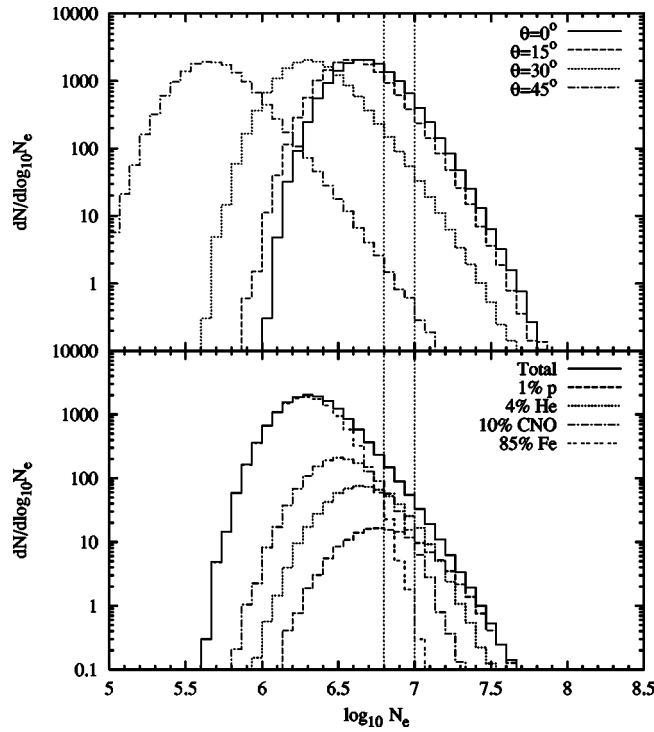


FIG. 8. Top panel: same as Fig. 4 for a primary cosmic ray composition consisting of 85% Fe, 10% CNO, 4% He and 1% protons. The bottom panel shows the $\theta=30^\circ$ size distribution that is plotted in the top panel illustrating how the different cosmic ray primaries contribute to build it up.

Figure 9 shows the ratio of the electron size distributions shown in the top panel of Fig. 8 for adjacent zenith angles. In the N_e range where the ratios are flat, they have numerical values very similar to the expected ratios for protons shown in Fig. 5 in the corresponding plateau regions, i.e. although the primary spectrum is dominated by heavy primaries the analysis method gives a value of the cross section similar to,

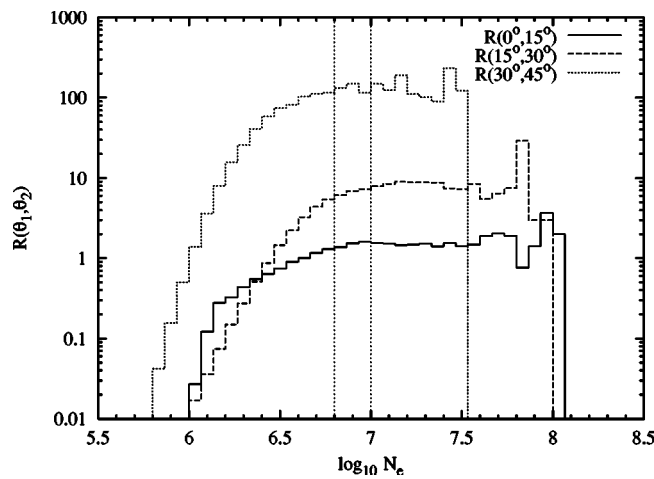


FIG. 9. Ratios of number of proton-initiated showers having between $10^{5.25}$ and $10^{5.45}$ muons and electron size N_e at 920 g/cm^2 as a function of N_e for a primary cosmic ray spectrum consisting of 85% Fe, 10% CNO, 4% He and 1% protons. Showers were simulated with SIBYLL 2.1.

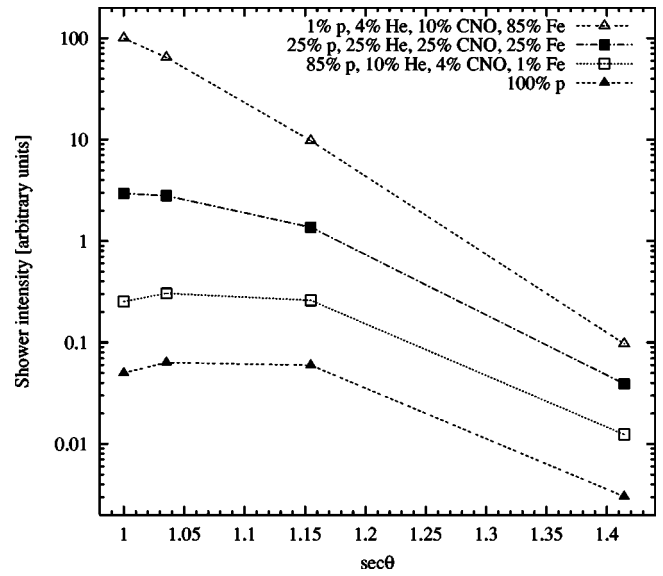


FIG. 10. Zenith angle dependence of the intensity of showers having constant $(\log_{10}N_\mu, \log_{10}N_e) = (5.25-5.45, 6.8-7.0)$ for different primary compositions. Showers were simulated with SIBYLL 2.1. The points are joined by straight lines to guide the eye. To avoid overlapping of the results for different compositions, they are multiplied by different arbitrary factors.

but somewhat higher than that obtained for pure protons.

The composition we chose in this analysis is completely “ad hoc.” In particular we have assumed an energy-independent ratio of the different elemental contributions. However, we have repeated the analysis for many different combinations of primary fractions, and only those with a large fraction of iron produce an exponential decrease of the intensity of showers with zenith angle. This is shown in Fig. 10.

We have not attempted to perform a fit to the intensity versus zenith angle using the different fractions of primaries as parameters in the fit. Such an analysis would require the use of a true detector Monte Carlo simulation and could only be performed by the experimental group. However from the combinations we have experimented with we conclude that at least 60–70% of iron is needed to produce a straight line in the nominal N_μ, N_e bin. The only way we can reproduce the experimental result is to assume that a large fraction of iron is present in the cosmic ray spectrum in the energy region between 10^{16} and 10^{17} eV. It is difficult to draw a more quantitative conclusion because of the differences of the muon number definitions of the experiment and in our calculations. We, however, obtain very similar results when using $\log_{10}N_e = 7.0-7.2$ bin, which may be closer to the showers selected by the Akeno experiment.

This conclusion is in qualitative agreement with recent analyses of the region around and above the knee in the cosmic ray spectrum (for example, KASCADE [17] and HiRes-MIA [18] measurements, see also [19]). Finally, we note that an early analysis [20] using the method of constant intensity cuts reached a similar conclusion about heavy composition in this energy range based on data from the BASJE air shower experiment on Mt. Chacaltaya [9].

IV. DISCUSSION AND CONCLUSIONS

We have investigated the influence of air shower fluctuations on the widely used constant intensity cut method. We consider two types of applications: the classic integral approach to the derivation of the cosmic ray energy spectrum and the differential N_μ, N_e cut used for the derivation of the proton-air cross section.

We find that the constant intensity cuts method can work for comparisons of data taken at different atmospheric depths and different angles. This is however possible only when the chemical composition of the primary cosmic rays is well known. The use of incorrect chemical composition can lead to a shift in the normalization of the energy spectrum. In the case of energy dependent composition the normalization errors for different cosmic ray flux components could also affect significantly the derived spectral index γ . Such shifts are also possible close to the detector N_e threshold, where measurements at different zenith angles would detect showers of different composition. The larger the zenith angle θ , the lighter would be the composition of the detected showers.

The influence of shower fluctuations is much bigger when the constant intensity cut is used in a differential way to compare showers with the same electron and muon sizes detected at different zenith angles. The selection by the muon size N_μ with constant intensity cuts is indeed a very good method and leads to a good angle independent energy selection. This is the result of the much slower absorption of the shower muons as well as the smaller N_μ fluctuations in showers with fixed primary energy.

The constant $N_e - N_\mu$ method, which is used for derivation of the proton-air production cross section, is dominated by fluctuations even in the case of a pure proton composi-

tion. The accuracy of this method improves with the selection of showers with large N_e for a fixed N_μ bin, where an experiment would run out of statistics. A possible improvement of the method would be to use Monte Carlo shower simulations to determine zenith angle dependent N_e bins. This, however, would represent a new method which is very different from the original idea of constant intensity cuts.

The Akeno data that were used for the derivation of the proton-air production cross section can be interpreted in terms of cosmic ray composition. The angle independent exponential slope of the shower absorption length indicates a substantial fraction of heavy primaries in the energy range of $10^{16} - 10^{17}$ eV. Because of the differences in the definitions of N_μ in the Monte Carlo results and those defined in Refs. [2,4] we cannot draw more definite quantitative conclusions based on the Monte Carlo results. We encourage the experimental group to update this analysis with the help of the new event generators, because the measurement of the cosmic ray chemical composition in this energy range is an important result. Our analysis of the experimental results in terms of cosmic ray composition demonstrated that the conclusions depend only mildly on the hadronic interaction model used in the simulation.

ACKNOWLEDGMENTS

We thank A.A. Watson for helpful discussions. J.A.O. is supported by CAPES ‘‘Bolsista da CAPES–Brasília/Brasil’’ and acknowledges Bartol Research Institute for its hospitality. This research is supported in part by NASA Grant NAG5-10919. R.E., T.K.G. and T.S. are also supported by the U.S. Department of Energy contract DE-FG02 91ER 40626. The simulations presented here were performed on Beowulf clusters funded by NSF grant ATM-9977692.

-
- [1] J. Alvarez-Muñiz *et al.* (in preparation).
 [2] T. Hara *et al.*, Phys. Rev. Lett. **50**, 2058 (1983).
 [3] R.M. Baltrusaitis *et al.*, Phys. Rev. Lett. **52**, 1380 (1984).
 [4] M. Honda *et al.*, Phys. Rev. Lett. **70**, 525 (1993).
 [5] M. Aglietta *et al.*, in *Proceedings of the 25th International Cosmic Ray Conference*, Durban, South Africa, 1997 (World Scientific, Singapore, 1997), Vol. 6, p. 37.
 [6] M. Aglietta *et al.*, in *Proceedings of the 26th Int’l Cosmic Ray Conference*, Salt Lake City, 1999 (AIP, Melville, NY, 2000), Vol. 1, p. 143.
 [7] M. Aglietta *et al.*, Nucl. Phys. B (Proc. Suppl.) **75A**, 222 (1999).
 [8] R.W. Ellsworth *et al.*, Phys. Rev. D **26**, 336 (1982).
 [9] H. Bradt *et al.*, in *Proceedings of the 9th International Cosmic Ray Conference*, London, 1965 (The Institute of Physics and the Physical Society, London, 1965), Vol. 2, p. 715.
 [10] M. Ave, J. Knapp, J. Lloyd-Evans, M. Marchesini, and A.A. Watson, astro-ph/0112253.
 [11] J. Alvarez-Muñiz, R. Engel, T.K. Gaisser, J.A. Ortiz, and T. Stanev, Phys. Rev. D **66**, 033011 (2002).
 [12] M. Nagano and A.A. Watson, Rev. Mod. Phys. **72**, 689 (2000).
 [13] R. Engel, T. K. Gaisser, P. Lipari, and T. Stanev, in *Proceedings of the 26th Int’l Cosmic Ray Conference*, Salt Lake City, 1999 (AIP, Melville, NY, 2000), Vol. 1, p. 415.
 [14] R. Engel, T. K. Gaisser, and T. Stanev, in *Proceedings of the 27th International Cosmic Ray Conference*, Hamburg, Germany, 2001 (Copernicus Gesellschaft, Katlemburg-Lindau, 2001), p. 431.
 [15] N.N. Kalmykov, S.S. Ostapchenko, and A.I. Pavlov, Nucl. Phys. B (Proc. Suppl.) **52B**, 17 (1997).
 [16] M. Nagano *et al.*, J. Phys. G **10**, 1295 (1984).
 [17] H. Ulrich *et al.*, in *Proceedings of the 27th International Cosmic Ray Conference*, Hamburg, Germany, 2001 (Copernicus Gesellschaft, Katlemburg-Lindau, 2001), p. 97.
 [18] T. Abu-Zayyad *et al.*, Astropart. Phys. **16**, 1 (2001).
 [19] S. P. Swordy *et al.*, Astropart. Phys. **18**, 129 (2002).
 [20] T. Gaisser, Nature (London) **248**, 122 (1974).
 [21] N.N. Nikolaev, Phys. Rev. D **48**, R1904 (1993).
 [22] R. Engel, T.K. Gaisser, P. Lipari, and T. Stanev, Phys. Rev. D **58**, 014019 (1998).
 [23] The measured mean free path corresponds to the particle production cross section. For a discussion of the difference between the inelastic and production cross sections in relation to air showers, see [21,22].